

# A passive nonlinear digital filter design which facilitates physics-based sound synthesis of highly nonlinear musical instruments

John R. Pierce and Scott A. Van Duyne

Center for Computer Research in Music and Acoustics, Stanford University, Stanford, California 94305

(Received 31 May 1996; revised 16 September 1996; accepted 17 September 1996)

Recent work has led to highly efficient physics-based computational models of wave propagation in strings, acoustic tubes, membranes, plates, and rooms using the digital waveguide filter, the 2-D digital waveguide mesh, and the 3-D tetrahedral digital waveguide mesh, all of which are suitable for real-time musical synthesis applications. A simple first-order nonlinear filter structure derived from a passive nonlinear impedance circuit is described which extends the usefulness of these models, and which avoids the difficulties of energy conservation when memoryless nonlinearities are inserted in resonant feedback systems. © 1997 Acoustical Society of America.

[S0001-4966(97)01602-0]

PACS numbers: 43.75.Tv [WJS]

## INTRODUCTION

Among the various approaches to the digital synthesis of musical sounds, some involve the production and excitation of linear resonances which are characteristic of a musical instrument. One fruitful notion has been that of considering the vibrating string as an electrical transmission line (Koch, 1937). The Karplus–Strong plucked-string algorithm (Karplus and Strong, 1983; Jaffe and Smith, 1983) models the vibrating string as a delay line loop. This is a special case of the traveling-wave-based digital waveguide modeling technique (Smith, 1992) which is applicable to many kinds of strings and acoustic tubes (Smith, 1987; Cook, 1990). The vibrating membrane and other two- and three-dimensional (2-D and 3-D) musical structures or reverberant environments have been modeled, and efficiently computed, using the multiply-free, parallel-computable, 2-D digital waveguide mesh (Van Duyne and Smith, 1993) and 3-D tetrahedral extension (Van Duyne and Smith, 1996). It is in the context of these kinds of wave-decomposed, computationally efficient digital modeling schemes that the current work on passive nonlinear filters most naturally resides.

While properly excited resonances of *linear* systems can closely approximate the tones of some musical instruments, *nonlinearity* plays an essential part in the sound of other musical instruments. Some nonlinearities are associated with the maintenance of oscillations in blown or bowed instruments (Smith, 1987). Others nonlinearities may be found in the excitation means of struck strings and percussion instruments, for example, the nonlinear compression force of piano hammer felt which leads to a greater spectral brightness of the sound with greater strike force (Chaigne and Askenfelt, 1994a, 1994b; Van Duyne *et al.*, 1994). The nature of the nonlinearity under present consideration is not to initiate, drive or maintain oscillation, but rather to modify the spectral energy distribution naturally and passively over time by transferring energy among resonating modes during the decay portion of the tone.

Fletcher and Rossing (1991) observe that after striking

cymbals, Chinese gongs, or tam-tams, the spectra become brighter with time. The higher portions of the spectra rise in comparison with the lower portions. The relative rise in higher frequencies, which is essential to the timbre of the sound, comes about because nonlinearities transfer vibrational energy from lower frequency to higher frequency modes. Beyond this, Lagge and Fletcher (1984) have shown that the compliance of a bridge supporting one end of a vibrating string can cause the transfer of energy among modes of vibration. Further, it has been known for some time that the flexible string is intrinsically nonlinear, except for the smallest vibrational amplitudes (Carrier, 1945). Thus, nonlinearities may have a smaller but nonetheless important effect on the tones of some stringed instruments.

We have found that the addition of passive nonlinearities to an otherwise linear digital synthesis algorithm can cause the transfer of energy among modes, and can lead to large and interesting alterations and evolutionary changes in timbre. In real physical instruments nonlinearities are necessarily passive because physical nonlinearities cannot cause an increase in total energy, but can only transfer energy among modes. The use of nonlinearities that are inherently passive in digital sound synthesis is important because other ways of adding nonlinearity can result in instability, oscillation, or unwanted energy loss.

A method has been found to incorporate an efficiently computable, energy conserving, first-order nonlinearity into a resonant feedback system. In particular, the first-order nonlinearity is a digital filter simulation of a spring which is stiffer for deflection in one direction than in the other, or alternatively, a capacitance which has a different value for positive than for negative voltages. Such an element stores no energy at zero deflection (spring) or at zero voltage (capacitor). Any energy that is stored by an increase in deflection or voltage will be given up as the deflection or voltage returns to zero. The element can store and release energy, but it cannot produce energy. The use or addition of this simple element is economical in computation and effective in causing energy transfer among otherwise linear modes. It can

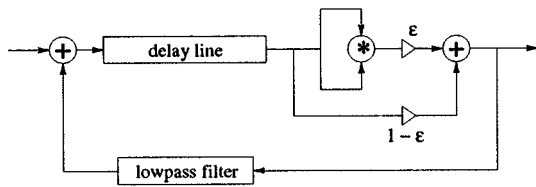


FIG. 1. Delay loop string model with square law nonlinearity.

lead to a substantial and pleasing alteration in the sound produced in an otherwise linear resonant feedback system. It has proven musically useful for both the qualitatively correct simulation of certain traditional instrument tones, and for the development of new and more exotic nonlinear synthetic tones.

## I. PROBLEM OVERVIEW

### A. Memoryless nonlinearity

Many spectral modifications, as occur during the time evolution of cymbal or gong tones, may be achieved by inserting *memoryless* nonlinearities into feedback loop systems. These kinds of nonlinearities have been used with success to induce auto-oscillation of feedback loops (Rodet, 1994). Nevertheless, energy conservation is out of control without additional amplitude tracking and/or scaling elsewhere in the loop. For example, Fig. 1 illustrates a simple nonlinear sound synthesis model based on the linear Karplus–Strong plucked-string algorithm (Karplus and Strong, 1983). The length of the delay line determines the fundamental pitch of the sound. The lowpass attenuation filter summarizes frequency-dependent loss per period in the string system. The simple linear loop model has been modified to include a square law nonlinearity within the feedback loop. The  $\epsilon$  and  $1 - \epsilon$  scalings allow some control over how much nonlinearity shall be present in the loop. The loop is linear for  $\epsilon$  set to 0. For small, nonzero  $\epsilon$ , a pleasant spectral brightening may occur over time. Interpreted physically, a memoryless scaling in the feedback loop may represent the transfer function at a terminating dashpot (or terminating resistor, in the transmission line case) between the left- and right-going traveling force waves (voltage waves). Figure 1 would then correspond to a string terminated on one end with a dashpot whose coefficient varies with the force applied to it, or to an oscillating transmission line terminated with a resistor whose coefficient depends on the voltage drop across it.

In Fig. 1, the choice of scaling coefficients,  $\epsilon$  and  $1 - \epsilon$ , will guarantee passivity of the system, understanding that the digital signal levels are restricted to between 1 and  $-1$ ; however, as we increase  $\epsilon$ , thereby increasing the amount of nonlinearity in the system, the nonlinear dashpot becomes more and more lossy. Yet, for important classes of musical instruments, such as gongs and cymbals, a large, nonlossy nonlinear effect is required. The scaling factors might be adjusted to allow more nonlinearity without as much loss by choosing, for example,  $\epsilon$  and  $1.1 - \epsilon$ , but this would correspond to a physical system where the terminating dashpot

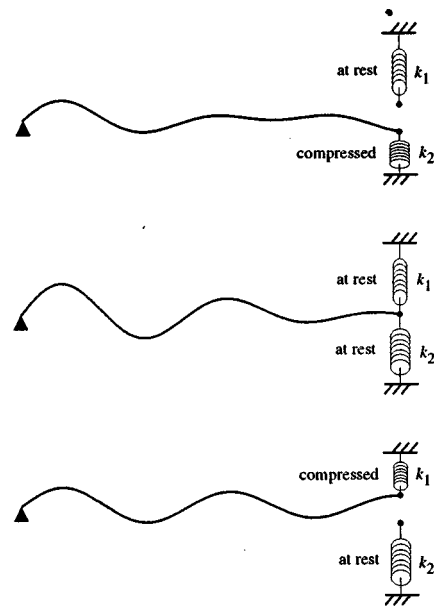


FIG. 2. String terminated with passive nonlinear double spring.

has an active impedance for certain forces and we risk instability in the loop without a careful monitoring of the overall loop gain.

In general, a memoryless nonlinearity may be formulated as a look-up table indexed by the samples of the incoming digital signal. There is no easy way to guarantee that the total energy of the input signal will equal the total energy of the output signal.

### B. First-order nonlinearity

In order to resolve this dilemma of having to trade off a musically desirable large nonlinear effect against the risk of system instability, while still maintaining a practical level of computational cost for real-time musical sound synthesis applications, the problem has been approached through the physical modeling of a passive nonlinear lumped termination impedance which has an internal state, that is, which is *not memoryless*. A passive nonlinear loop filter has been derived based on a real physical system constructed from passive, lossless elements only, namely, two springs of differing stiffness.

Consider a string terminated by a double-spring apparatus as shown in Fig. 2. Three states of the system are shown in the figure: First, the lower spring is compressed, while the upper spring is at rest; second, both springs are at rest; and, third, the upper spring is compressed, while the lower spring is at rest. In effect, the spring termination apparatus is equivalent to a single nonlinear spring whose stiffness constant is  $k_1$  when the displacement is positive and  $k_2$  when the displacement is negative.

Now consider what is happening to the energy in the system. When the lower spring is compressed, some energy from the string is converted to potential energy stored in the spring. When the lower spring returns to its rest state, the stored spring energy is entirely returned to the string, and the spring contains no stored energy. When the upper spring is

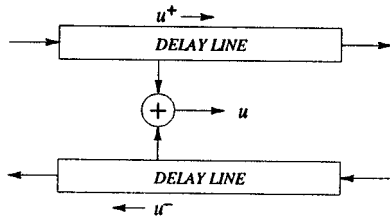


FIG. 3. The digital waveguide.

then compressed, exactly the same kind of energy exchange occurs. This ideal system is physically passive and lossless since energy is neither created nor destroyed.

If the spring stiffness constant had changed while stored potential energy was still in the spring, i.e., when one of the springs was still compressed, the stored energy would be scaled by the new relative stiffness of the spring. In this case, the stored energy before the stiffness change would be different from the stored energy after the stiffness change, leading to the creation or loss of energy, possibly resulting in a nonpassive system. In any model of this nonlinear system, care must be taken to change the spring stiffness coefficient at the right time in order to preserve passivity and losslessness.

Passivity is the requirement that no energy be created by the system. When energy is created in a feedback loop, stability problems may ensue. We have specifically tried to discover a nonlinear system which is passive, and which is lossless, so the system loss may be decoupled from the nonlinear effect, and designed separately.

## II. NONLINEAR FILTER DERIVATION

### A. The digital waveguide string model

The one-dimensional wave equation may be solved as the sum of two waves traveling in opposite directions (Morse and Ingard, 1968). The traveling wave solution has led to the digital modeling of string and acoustic tube oscillations using a pair of bi-directional delay lines, each delay line implementing one of the traveling waves. This efficient filter structure is known as the digital waveguide (Smith, 1992, 1987). The traveling may represent displacement, velocity, slope, force, or other physical variables. Traveling waves are mathematical constructs, the actual physical values at any point on the string being the sum of the right- and left-going traveling components at that point. Figure 3 illustrates a physical variable,  $u$ , as the sum of its traveling components,  $u^+$  and  $u^-$ , at some point on the waveguide. The delay lines represent both a sampled delay in time and a sampled position in space. The digital waveguide filter structure permits an exact band-limited reconstruction of the continuous traveling wave in time and space.

If transverse velocity or displacement waves on a string are being modeled, then, on reaching a rigid termination, the traveling wave in the right-going delay line will invert and turn into the left-going delay line. This is to say that the velocity wave transfer function at a rigid termination is  $-1$ . Similarly, if transverse force waves are being modeled, then the force wave transfer function at a rigid termination is  $+1$ ,

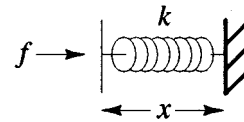


FIG. 4. Simple linear spring system.

that is, there is no inversion of force waves at a rigid termination. The case of a springy termination is considered below.

There is a *wave impedance* relationship between the traveling components of force and velocity in the string, corresponding to the wave impedance relation between pressure and flow in acoustic tubes, or voltage and current in electrical transmission lines (Magnusson, 1970), which can be written

$$f^+ = R_0 v^+ \quad \text{and} \quad f^- = -R_0 v^-, \quad (1)$$

where  $f^\pm$  and  $v^\pm$  are the traveling wave components of force and velocity, respectively, and where the wave impedance is  $R_0 = \sqrt{K\epsilon}$ ,  $K$  being the constant tension on the string and  $\epsilon$  being the mass density per unit length. Intuitively, these equations say that when a force is applied transversely to a string, the resultant transverse velocity should be less for greater string mass and for greater string tension. The change in sign for the left-going components is due to coordinate system choice. Note that no matter whether velocity or force waves are being modeled in the system loop, both physical force and physical velocity at any point along the string may be computed from the resident traveling wave components using Eq. (1) to make the change of variables,

$$v = v^+ + v^- = (1/R_0)(f^+ - f^-), \quad (2)$$

$$f = f^+ + f^- = R_0(v^+ - v^-). \quad (3)$$

### B. The linear spring termination

The force equation for the ideal linear spring shown in Fig. 4 is

$$f(t) = kx(t) \Rightarrow \frac{df(t)}{dt} = kv(t), \quad (4)$$

where  $f(t)$  is the force applied on the spring at time  $t$ ,  $x(t)$  is the compression distance of the spring,  $v(t)$  is the velocity of compression, and  $k$  is the spring stiffness constant.

Taking the Laplace transform mapping  $f(t)$  to  $F(s)$  and  $v(t)$  to  $V(s)$ , and further assuming no initial force on the spring, we get

$$F(s) = (k/s)V(s). \quad (5)$$

Here,  $k/s$  is the lumped impedance of the spring. Setting  $s = j\omega$  will give the frequency response of this system.

Figure 5 shows a string terminated by a spring. As was suggested in Eqs. (2) and (3), the physical force at the string termination is the sum of the transverse force waves on the string at that point,  $f = f_r + f_l$ , while the physical velocity at the termination is the difference between the force waves scaled by  $1/R_0$ ,  $v = (1/R_0)(f_r - f_l)$ . We may, therefore, reformulate Eq. (5) as a transfer function from  $F_r$  to  $F_l$ ,

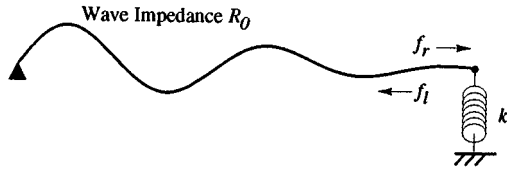


FIG. 5. String terminated by simple spring.

$$F(s) = (k/s)V(s), \quad (6)$$

$$F_r(s) + F_l(s) = \left(\frac{k}{s}\right) \frac{F_r(s) - F_l(s)}{R_0}, \quad (7)$$

$$F_l(s) = \frac{k/s - R_0}{k/s + R_0} F_r(s). \quad (8)$$

The force wave transfer function is stable allpass since its pole is at  $s = -k/R_0$  and its zero is at  $s = k/R_0$ , where  $k$  and  $R_0$  are defined to be positive real numbers.

### C. Moving to the digital domain

While it is appropriate simply to sample the continuous traveling waves to form the digital waveguide filter structure, it is convenient to make a conformal bilinear transform when taking the spring system from the  $s$  plane to the  $z$  plane (Parks and Burrus, 1987; Nehari, 1952),

$$s \leftarrow \alpha \frac{1 - z^{-1}}{1 + z^{-1}}. \quad (9)$$

This bilinear transform maps DC in the continuous system to DC in the digital system, while mapping infinite frequency in the continuous system to half the sampling rate, or the Nyquist limit frequency, in the digital system. Further, the system retains its allpass characteristics, which is essential for the present purpose. The parameter  $\alpha$  is a degree of freedom which may be used to control the frequency warping. It is usual to choose  $\alpha = 2/T$  to obtain faithful frequency response at the low end of the frequency range (Parks and Burrus, 1987).

The bilinear transform is applied to Eq. (8) to obtain

$$F_l(z) = H(z)F_r(z), \quad (10)$$

where

$$H(z) = \frac{a_0 + z^{-1}}{1 + a_0 z^{-1}} \quad \text{and} \quad a_0 = \frac{k - \alpha R_0}{k + \alpha R_0}. \quad (11)$$

The filter coefficient  $a_0$  ranges from  $-1$  to  $1$  as the spring stiffness parameter  $k$  ranges from  $0$  to  $\infty$ . The frequency domain transfer function, Eq. (10), corresponds to a time domain difference equation of the form

$$f_l(n) = a_0 f_r(n) + f_r(n-1) - a_0 f_l(n-1), \quad (12)$$

where  $n$  is the sampled time index. Figures 6 and 7 show two alternative implementations of this allpass difference equation. The  $z^{-1}$  blocks indicate a delay of one time sample.

Since the filter coefficient,  $a_0$ , represents the spring stiffness, only  $a_0$  need be changed to modify the stiffness of the spring termination. However, to preserve physical and digital

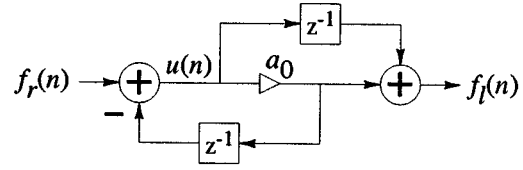


FIG. 6. Allpass filter implementation.

passivity and losslessness this change must be made just at the point where the spring passes through its rest position.

### D. Physically correct coefficient modulation

Consider the internal filter signal  $u(n)$  in the allpass filter implementation of  $H(z)$  shown in Fig. 6. From the diagram, it may be seen that

$$f_l(n) = a_0 u(n) + u(n-1), \quad (13)$$

$$u(n) = f_r(n) - a_0 u(n-1). \quad (14)$$

The actual physical force applied to the spring termination is equal to the sum of the input and output force waves, as defined in Eq. (3). Using (13) and (14), an expression of the actual force on the spring,  $f(n)$ , may be found:

$$f(n) \triangleq f_r(n) + f_l(n) \quad (15)$$

$$= (1 + a_0)[u(n) + u(n-1)]. \quad (16)$$

Equation (16) indicates that the actual physical force on the spring is proportional to a linearly interpolated value of signal  $u$  at time  $n-0.5$ . From Eq. (4), displacement of the spring termination is zero when force is zero, and  $f(n)$  is zero when  $u(n) + u(n-1)$  is zero. Therefore, when  $u$  changes sign between times  $n-1$  and  $n$ , the spring displacement is closest to zero. Hence, this is as close as we can get to the physically correct time to change the spring stiffness coefficient in order to model the nonlinear spring termination system shown in Fig. 2.

In some computational circumstances, the alternative filter structure shown in Fig. 7 may be preferable to that in Fig. 6. From the diagram in Fig. 7, it may be seen that

$$f_l(n) = w(n-1) + a_0 f_r(n), \quad (17)$$

$$w(n) = f_r(n) - a_0 f_l(n). \quad (18)$$

Combining (17) and (18) as before, the termination force may be found:

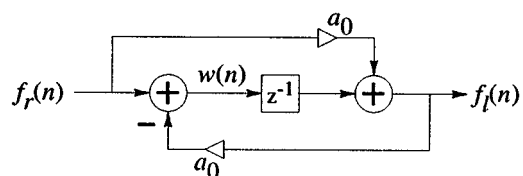


FIG. 7. Alternative allpass filter implementation.

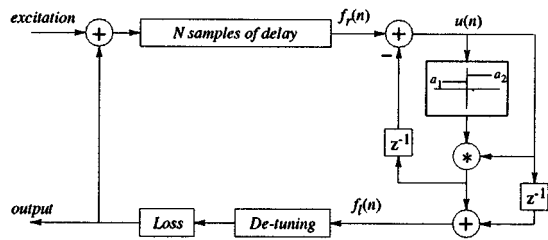


FIG. 8. Nonlinear string/spring system.

$$f(n) \triangleq f_r(n) + f_f(n) \quad (19)$$

$$= \left( \frac{1}{1-a_0} \right) [w(n) + w(n-1)], \quad (20)$$

and the same arguments apply as above. The physically correct time to change the allpass filter coefficient is when the spring force is nearest to zero, which is when the state signal,  $w(n)$ , changes sign.

### E. Digitally correct coefficient modulation

The internal filter state signal,  $u(n)$  in Fig. 6, or  $w(n)$  in Fig. 7, represents the digital energy stored in the filter at any given time,  $n$ . Assume that the allpass coefficient  $a_0$  is to be changed at time  $n = T_c$ . Also, assume that there is no input signal after time  $T_c$ , i.e.,  $f_r(n) = 0$  for  $n > T_c$ , and that there is some nonzero internal state value at time  $n = T_c$ . Then the output of the filter caused only by this internal energy state value is proportional to the decaying exponential,  $a_0^{n-T_c}$ , and the corresponding energy is the sum of squares of this output signal.

If the coefficient,  $a_0$ , is suddenly changed at time  $n = T_c$ , it is clear that the internal state energy will ring out of the filter with a different decay rate than if the coefficient had not been changed, and hence, the energy will not be conserved. Such coefficient changes, if made arbitrarily, may lead to instability in a feedback loop. However, if the internal state,  $u(T_c)$  for Fig. 6, or  $w(T_c)$  for Fig. 7, is zero or near zero when the coefficient  $a_0$  is changed, then the resultant discontinuity in the state energy will be minimal or zero. Therefore, to maintain the desired passivity in the nonlinear allpass filter, the filter coefficient change is gated on the sign of the state. This method of gating the coefficient change is both *physically correct*, since when the state is near zero, the modeled force on the element is correspondingly near zero, and *digitally correct*, since it minimizes energy discontinuities arising from the internal state.

Figure 8 shows a digital system diagram for the nonlin-

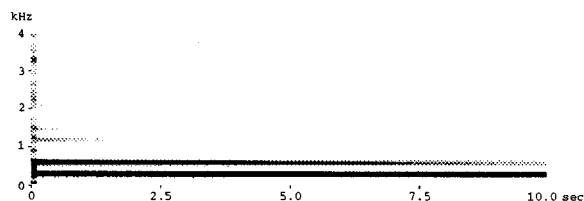


FIG. 9. Spectrogram of harmonic loop with lowpass filter.

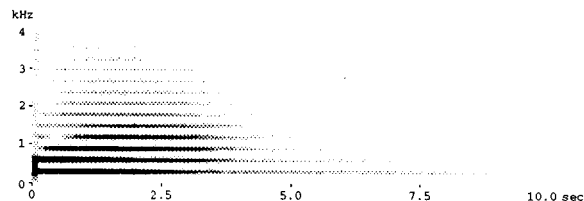


FIG. 10. Spectrogram of harmonic loop with lowpass filter and passive nonlinear filter.

ear string/spring system of Fig. 2 using the allpass filter variant given in Fig. 6. For graphical convenience, a look-up table notation is used to show how  $u(n)$  gates the coefficient change, but, in general, this would be implemented in simple conditional logic. Also shown in the loop are a delay line block which determines the fundamental pitch of the loop, a loss filter block which generally is a lowpass filter used to model a frequency dependent attenuation per period, and a detuning filter block representing some static allpass filters which may make a fractional sample delay correction or, otherwise, introduce inharmonicities into the loop.

### III. MUSICAL EXAMPLES

The passive nonlinear filter was tested in a variety of musical situations. Shown here are comparisons of the spectral evolution, with and without nonlinearity, of two sounds generated by essentially the model in Fig. 8. In the first example, Fig. 9 shows the spectral evolution of a simple delay line plus lowpass filter loop excited in such a way that the third harmonic is highly attenuated, and in which the nonlinear filter is deactivated. We see a natural exponential decay with higher frequency modes decaying faster than low frequency modes. In Fig. 10, the passive nonlinear filter has been activated with the result that the spectrum brightens over time; in particular, the initially missing spectrum third harmonic builds up energy, as do several higher harmonics. After a few seconds, the effect of the lowpass filter in the loop takes over and the loop decays out.

In a second example, the same system is used with the addition of an allpass filter in the loop to detune the modes slightly, giving it a more bell-like tone. Figure 11 shows the spectral evolution when the nonlinear filter is deactivated. Figure 12 shows the result when the nonlinear filter is operating. Note that the modes exchange energy among themselves in a more dynamic manner in this inharmonic case.

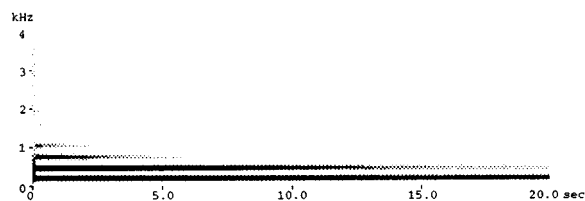


FIG. 11. Spectrogram of inharmonic loop with lowpass filter.

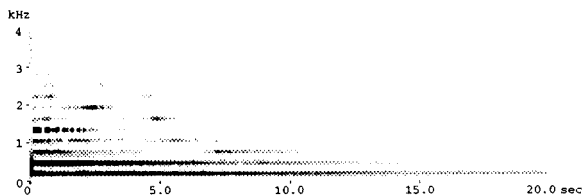


FIG. 12. Spectrogram of inharmonic loop with lowpass filter and passive nonlinear filter.

In addition to these simple loop cases, promising gong- and cymbal-like sounds have been generated by incorporating these passive nonlinear filters into the 2-D digital waveguide mesh membrane model (Van Duyne and Smith, 1993; Van Duyne *et al.*, 1994).

#### IV. PHASE MODULATION ANALYSIS

The time-varying allpass termination filter shown in Fig. 8 is essentially lossless and passive. However, for it to be useful it must behave in the desired manner. Energy in existing resonant modes of the main system must be caused to spread locally in the spectrum to nearby modes of the system, as is observed in real musical instruments (Fletcher and Rossing, 1991). Empirically, this seems to happen, as seen in Figs. 9–12. However, this filter is difficult to analyze strictly, due to its signal-dependent time variation and due to its inclusion in a feedback loop system. Nonetheless, an intuitive understanding of its operation may be gleaned by considering a simpler, but nonpassive, form.

The termination filter in Fig. 8 is a one-pole allpass filter with a time-varying coefficient. Consider the frequency response of an allpass filter of the same form with a *sinusoidally* varying coefficient taking on values between  $a_1$  and  $a_2$ . Intuitively, this filter will be performing a phase modulation on the input signal. Hence, the output signal of the filter should contain sidebands generated by this phase modulation at multiples of the modulation frequency. Figure 13 shows the dB magnitude spectrum of the output signal of this filter with an input sine wave “center frequency” of 8000 Hz and a coefficient “modulating frequency” of 2000 Hz. The resultant sidebands of the output signal are just as expected.

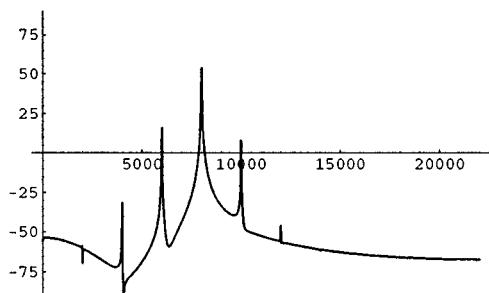


FIG. 13. Output dB magnitude spectrum of sinusoidally driven allpass filter with sinusoidally modulated coefficient.

Modulating the coefficient,  $a_0(n)$ , with a square wave, instead of a sine wave, should result in an output signal spectrum containing some greater emphasis in the odd sidebands, due to the odd harmonics in the square wave coefficient modulation signal.

In the passive nonlinear filter form of Fig. 8, where the coefficient change is controlled by the change in sign of the internal signal,  $u(n)$ , the modulating signal is quasi-square wave in that it flips between two distinct values, and it has a “fundamental frequency” related to the input signal to the filter, since  $u(n)$  is just a filtered version of the input signal,  $f_r(n)$ , as indicated in Eq. (14). The filter output signal will, therefore, contain sidebands corresponding to sum and difference frequencies of the input signal, generally grouping near frequencies in the input signal. Further, the choice of  $a_1$  and  $a_2$  may be used to determine the rate of energy spreading and the spectral region where it is most active, by simple analysis of the relative phase response variation between the first-order allpass filters with these two coefficients.

For coupling to occur in the resonant system, the sidebands produced by the modulated allpass filter must fall on supported modes of the system. When a sideband coincides with a supported mode, that mode will be driven by the energy from the appropriate sideband. Energy from sidebands which do not fall on supported modes will not drive any particular mode and will simply be absorbed back into the system. Since the passive nonlinear filter produces sum and difference frequencies of the input signal, we can expect that at least some of the main system modes will be hit and energy spreading will occur.

#### V. CONCLUSIONS

A first-order, physically motivated, nonlinear digital filter has been developed which is passive and energy conserving. It may be incorporated easily into linear resonant filter-based sound synthesis algorithms such as the Karplus–Strong plucked-string algorithm, and the various one-, two-, and three-dimensional digital waveguide filter structures. The nonlinear effect is pleasing, natural, and qualitatively similar to that which may be observed in real musical instruments, namely, a gradual spreading of spectral energy from existing modes to their neighbor modes. The rate of energy spreading and spectral region of greatest activity may be tuned using the two filter parameters. The filter is computationally efficient and suitable for real-time sound synthesis applications.

- Carrier, G. F. (1945). “On the non-linear vibration problem of the elastic string,” *Q. Appl. Math.* **3**, 157–165.
- Chaigne, A., and Askenfelt, A. (1994a). “Numerical simulations of piano strings. I. A physical model for a struck string using finite difference methods,” *J. Acoust. Soc. Am.* **95**, 1112–1118.
- Chaigne, A., and Askenfelt, A. (1994b). “Numerical simulations of piano strings. II. Comparisons with measurements and systematic exploration of some hammer-string parameters,” *J. Acoust. Soc. Am.* **95**, 1631–1640.
- Cook, P. R. (1990). *Identification of Control Parameters in an Articulatory Vocal Tract Model*, with Applications to the Synthesis of Singing, Stanford Univ. Music Dept., Center for Computer Research in Music and Acoustics, Report No. STAN-M-68.
- Fletcher, N. H., and Rossing T. D. (1991). *The Physics of Musical Instruments* (Springer-Verlag, New York).

- Jaffe, D. A., and Smith, J. O. (1989). "Extensions of the Karplus–Strong plucked-string algorithm," in *The Music Machine*, edited by C. Roads (MIT, Cambridge, MA), reprinted from *Comput. Music J.* **7**(2) (1983).
- Karplus, K., and Strong, A. (1989). "Digital synthesis of plucked-string and drum timbres," in *The Music Machine*, edited by C. Roads (MIT, Cambridge, MA), reprinted from *Comput. Music J.* **7**(2) (1983).
- Kock, W. E. (1931). "The vibrating string considered as an electrical transmission line," *J. Acoust. Soc. Am.* **8**, 227–233.
- Lagge, K. A., and Fletcher, N. H. (1984). "Nonlinear generation of missing modes on a vibrating string," *J. Acoust. Soc. Am.* **76**, 5–12.
- Magnusson, P. (1970). *Transmission Lines and Wave Propagation* (Allyn and Bacon, Boston).
- Morse, P., and Ingard, K. (1968). *Theoretical Acoustics* (McGraw-Hill, New York).
- Nehari, Z. (1952). *Conformal Mapping* (McGraw-Hill, New York).
- Parks, T. W., and Burrus, C. S. (1987). *Digital Filter Design* (Wiley, New York).
- Rodet, X. (1994). "Stability/instability of periodic solutions and chaos in physical models of musical instruments," *Proc. International Computer Music Conference* (Århus, 1994).
- Smith, J. O. (1992). "Physical modeling using digital waveguides," *Comput. Music J.* **16**(4).
- Smith, J. O. (1987). *Music Applications of Digital Waveguides*, Stanford Univ. Music Dept., Center for Computer Research in Music and Acoustics, Report No. STAN-M-39.
- Van Duyne, S. A., and Smith, J. O. (1996). "The 3D tetrahedral digital waveguide mesh with musical applications," *Proc. International Computer Music Conference* (Hong Kong, 1996).
- Van Duyne, S. A., Pierce, J. R., and Smith, J. O. (1994). "A passive nonlinear mode-coupling circuit and the wave digital hammer," *Proc. International Computer Music Conference* (Århus, 1994).
- Van Duyne, S. A., and Smith, J. O. (1993). "Physical modeling with the 2D digital waveguide mesh," *Proc. International Computer Music Conference* (Tokyo, 1993).